An Active Islanding Detection Method for Small-Scale Distributed Generators

WEN-YEAU CHANG
Department of Electrical Engineering
St. John's University
No. 499, Sec. 4, Tam King Road, Tamsui, Taipei 251, Taiwan
TAIWAN
changwy@mail.sju.edu.tw

Abstract: - This paper proposes a new islanding detection method for use in a small-scale, grid-interconnected distributed generator system. The proposed islanding detection method is based on voltage fluctuation injection, which can be obtained through high-impedance load switching on the grid periodically. The correlation factor between the periodic switching signal and the perturbed voltage is then used as an islanding detection index in the proposed islanding detection method. Experimental results demonstrate the principles of the proposed technique and show the new proposed method is reliable, economical, and easy to implement.

Key-Words: - Islanding detection, Distributed generator, Voltage fluctuation injection, Correlation factor

1 Introduction

Distributed generator (DG) is defined as the generator of power inside the distribution system. DG is driven by prime movers such as a wind turbine, water turbine, micro-turbine, etc. to generate electricity. Due to the technological innovations related to the energy conversion in the last decade, it is now possible to have competitive electricity generation with DG units. Many papers have been presented in literature regarding the sizing, placement, reliability, and expansion planning of DG [1-3]. The main merits of DG can be listed as follows: reduction of power loss, voltage profile improvement, power quality improvement (in some cases), possibility to exploit CHP (Combined Heat and Power) generation, less polluting emissions (with respect to traditional plants) [4]. Since DG is inside the distribution system, it changes the characteristics of the distribution system, causing an impact in the voltage regulation and protection scheme [5-8].

An essential requirement of the grid-interconnected DG system is the capability of islanding detection [9]. Islanding occurs when a part of the distribution system is electrically isolated from the main source of supply, yet continues to be energized by DG. The islanding operation of DG may cause potential hazards to line-maintenance personnel, and risk the DG in being damaged by out-of phase reconnection to the grid. The majority of utilities require that DG should be disconnected from the grid as soon as the islanding occurs. IEEE standard 1547 stipulates a maximum delay of 2 seconds for detection of an islanding [10].

The islanding detection methods can be generally categorized into two groups, passive methods and active methods. Passive methods detect the islanding operation of DG by monitoring selected power system parameters, such as voltage magnitude, the change rate of frequency, phase displacement, and power output. The passive methods include the change of voltage magnitude relay [11], the rate of change of frequency relay [12], the vector surge relay [13], the voltage unbalance and total harmonic distortion of current relay [14], the change of output power relay [15], the ratio of the frequency change to the output power change relay [16], the rate of change of voltage and power factors relay [17], and the logical rule-based detection technique [18]. The principles of these methods were developed based on the fact that an islanding will cause variations in system parameters. However, when the amount of power mismatch between the DG and local load is not significant enough during islanding, the methods mentioned above may fail to signal the abnormality. Besides, another drawback to the passive methods is that they cannot effectively differentiate between the islanding and other non-islanding transients, like voltage flicker or sag.

Active methods detect the islanding by directly interacting with the system under consideration. The three main methods are the reactive error export detection (REED) [19], the positive feedback for power loop method [20], and the voltage fluctuation

correlated method [21]. The REED controls the excitation current of DG so that it generates a known value of reactive current, which cannot be supported unless the generator is connected to the grid [19]. The positive feedback for power loop method will result in an unstable frequency or voltage, once the DG is islanded. Eventually, the unstable frequency or voltage will trip the frequency or voltage relay to protect islanding [20]. The small-scale DG has simple excitation, perhaps using permanent magnets. Hence, islanding of small-scale DG cannot be detected effectively by controlling the reactive power export, as in REED or the positive feedback for power loop method.

Another method is called the voltage fluctuation correlated method [21]. Using power transistor switching high-impedance load periodically near the voltage zero crossing point, it measures the voltage fluctuation through the utility-interconnected point, enabling evaluation of system source impedance and detection of islanding. It provides a very effective means of detection, with the disadvantage of introducing a small voltage perturbation at the zero crossing point. Active methods are more effective and robust than the passive ones, but most existing active schemes have the disadvantages of high cost and degradation of power quality to a certain extent.

To overcome the disadvantages of the existing islanding detection methods, the aim of this paper is to propose a new correlation factor islanding detection method for small-scale, typically less than 1 kW, grid-interconnected DG. The proposed method is more effective and economical than conventional active methods, and has very little impact on the power quality.

2 Basic Principle of the Proposed Method

The proposed islanding detection method is based on the feature that the variation at the terminal voltage of DG has a strong correlation with its voltage perturbation source when DG is operating in islanding state. On the contrary, the variation at the terminal voltage of DG has a weak correlation with its voltage perturbation source when DG is operating in parallel with the grid. Therefore, measuring the correlation between variation at terminal voltage and its voltage perturbation source would show whether the DG is operating in parallel with the grid or functioning independently of the grid. In the proposed islanding detection applications, a periodically switching high-impedance load is used, so that variation of load voltage is restricted to the level, which would not influence the supply.

The equivalent circuit of a DG parallel with the grid in normal operation is shown in Fig. 1, where E_u and E_g are the open circuit voltages of the utility and the DG; Z_u is the source impedance of the utility grid; Z_g is the internal impedance of DG; Z_L is the impedance of the local load; Z_h is the impedance of the high-impedance load; S is the periodical switch of Z_h. The terminal voltage of grid-interconnected point when S is turn-off can be expressed as:

$$V_{L1} = \left(\frac{Z_g E_u}{Z_u + Z_g} + \frac{Z_u E_g}{Z_u + Z_g}\right) \times \frac{Z_L}{Z_L + \dfrac{Z_u Z_g}{Z_u + Z_g}} \qquad (1)$$

Since Z_g is significantly greater than Z_u for distribution system, even for the long radial system or the weak grid system [21], $\dfrac{Z_g E_u}{Z_u + Z_g}$ term is significantly greater than $\dfrac{Z_u E_g}{Z_u + Z_g}$ term in (1). If the $\dfrac{Z_u E_g}{Z_u + Z_g}$ term is ignored, V_{L1} can be approximately expressed as:

$$V_{L1} \cong \frac{Z_g E_u}{Z_u + Z_g} \times \frac{Z_L}{Z_L + Z_u} \cong E_u \times \frac{Z_L}{Z_L + Z_u} \qquad (2)$$

The terminal voltage of grid-interconnected point when *S* is turn-on can be expressed as:

$$V_{L1}^{'} = \left(\frac{Z_g E_u}{Z_u + Z_g} + \frac{Z_u E_g}{Z_u + Z_g}\right) \times \frac{\dfrac{Z_L Z_h}{Z_L + Z_h}}{\dfrac{Z_L Z_h}{Z_L + Z_h} + \dfrac{Z_u Z_g}{Z_u + Z_g}} \qquad (3)$$

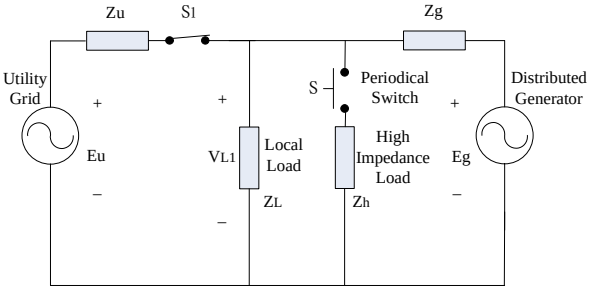

Fig. 1 Equivalent circuits of a DG parallel with the grid

If the $\frac{Z_u E_g}{Z_u + Z_g}$ term is ignored, $V_{L1}^{'}$ can be approximately expressed as:

$$V_{L1}^{'} \cong \frac{Z_g E_u}{Z_u + Z_g} \times \frac{\frac{Z_L Z_h}{Z_L + Z_h}}{\frac{Z_L Z_h}{Z_L + Z_h} + Z_u}$$

$$\cong E_u \times \frac{\frac{Z_L Z_h}{Z_L + Z_h}}{\frac{Z_L Z_h}{Z_L + Z_h} + Z_u} \quad (4)$$

The variation at terminal voltage due to the S switching can be approximately expressed as:

$$\Delta V_{L1} = V_{L1} - V_{L1}^{'}$$

$$= E_u \times \frac{Z_L}{Z_L + Z_u} - E_u \times \frac{\frac{Z_L Z_h}{Z_L + Z_h}}{\frac{Z_L Z_h}{Z_L + Z_h} + Z_u} \quad (5)$$

The equivalent circuit of a DG subject to islanding operation is shown in Fig. 2. The terminal voltage of grid-interconnected point when S is turn-off can be expressed as:

$$V_{L2} = E_g \times \frac{Z_L}{Z_g + Z_L} \quad (6)$$

The terminal voltage of grid-interconnected point when *S* is turn-on can be expressed as:

$$V_{L2}^{'} = E_g \times \frac{\frac{Z_L Z_h}{Z_L + Z_h}}{\frac{Z_L Z_h}{Z_L + Z_h} + Z_g} \quad (7)$$

The variation at terminal voltage due to the S switching can be approximately expressed as:

$$\Delta V_{L2} = V_{L2} - V_{L2}^{'}$$

$$= E_g \times \frac{Z_L}{Z_L + Z_g} - E_g \times \frac{\frac{Z_L Z_h}{Z_L + Z_h}}{\frac{Z_L Z_h}{Z_L + Z_h} + Z_g} \quad (8)$$

Since the internal impedance of DG (Z_g) is significantly greater than the source impedance of utility (Z_u), comparing (8) with (5), we have ΔV_{L2} is larger than ΔV_{L1}. Variation at the terminal voltage due to the switching of the high-impedance load during islanding operation is thus larger than that in normal operation.

The experimental system was performed, and the results are shown in Figs. 3 to 4. The DG employed in the tests consisted of a grid-interconnected, three-phase, 220V, 300W synchronous generator and a 2000Ω high-impedance inductive load. As an example of the typical test for the DG in normal operation, Fig. 3 exhibits that the variation at the terminal voltage due to the switching of the high-impedance load is very small. The frequency in the terminal voltage is 60Hz, and the frequency of the switching signal is 10Hz.

As an example of the typical test for the DG in islanding operation, Fig. 4 exhibits that the variation at the terminal voltage due to the switching of the high-impedance load in islanding operation is larger than that in normal operation. In Figs. 3 to 4, Channel 1 denotes the waveform of the terminal voltage (100V/div), Channel 2 indicates the waveform of the switching signal of the high-

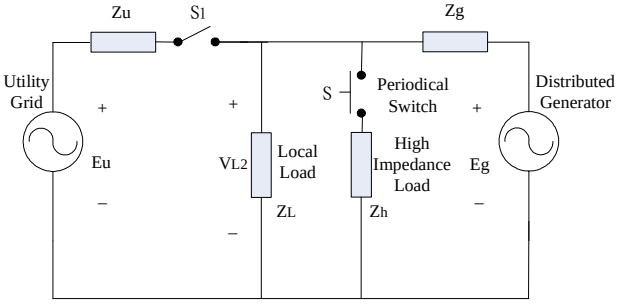

Fig. 2 Equivalent circuits of a DG during islanding operation

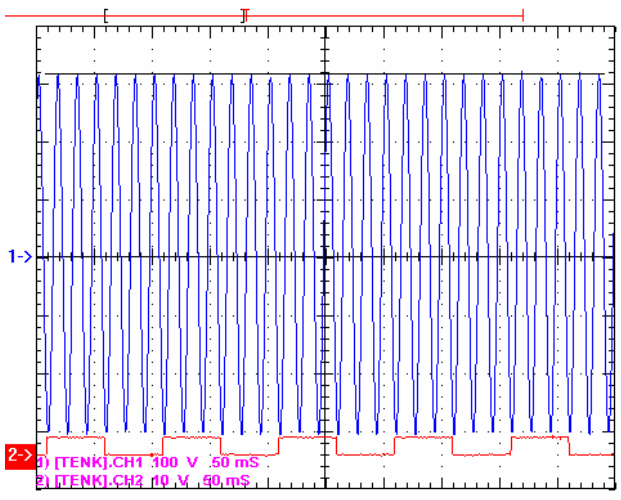

(1)CH1:100V/div (2)CH2:10V/div Time:50ms/div

Fig. 3 Waveform of terminal voltage and switching signal during normal operation

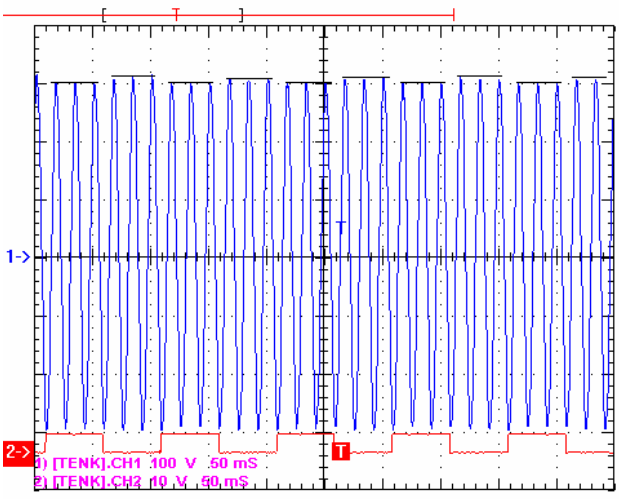

(1)CH1:100V/div (2)CH2:10V/div Time:50ms/div

Fig. 4 Waveform of terminal voltage and switching signal during islanding operation

impedance load (10V/div).

Measuring the periodical perturbation of terminal voltage at the grid-interconnected point, due to switching a known high-impedance load, allows one to estimate indirectly the DG operating state. When the variation at the terminal voltage changed, the islanding operation can be easily detected accordingly.

However, variations in the terminal voltage may result from some load switching, other than the switching of the high-impedance load. Consequently, to avoid false alarms, the measured variation of terminal voltage should be closely related with the given high-impedance load switching signal as in the islanding operation. Nevertheless, in the case of some load changes occurring coincidentally with the intentional high-impedance load switching, the measured voltage fluctuation may not represent the supply impedance change. Distinction between intentional and coincidental load changes should be made by observing a number of more switching instances and terminal voltage changes [21]. To effectively distinguish variations of the terminal voltage due to switching of the given high-impedance load from the others should thus be based on correlation of the measured terminal voltage changes with the given load switching.

3 The Proposed Detection System

The architecture of the proposed correlation factor detection system is illustrated in Fig. 5. The insulated gate bipolar transistor based periodical electronic switching circuit performs the high-impedance load switching. A voltage detecting interface measures the magnitude of terminal voltage at the grid-interconnected point. The digital signal processor calculates the correlation factor between the periodical switching signal and the perturbed voltage at the grid-interconnected point and decides whether the trip conditions are met.

At the zero crossing point of the terminal voltage, the periodical electronic switching circuit turns on/off every three cycles. The voltage fluctuation due to the periodical switching in an islanding operation would be significantly greater than that in the normal operation. Since the periodical electronic switch turns on/off every three cycles, the switching signal $S(j)$ has a period of six cycles. $S(j)$ has two values, -1 for turn-on status and +1 for turn-off status. The differential signal $\Delta S(j)$ of $S(j)$ with 3-cycle time lag is described as follows:

$$\Delta S(j) = S(j) - S(j-3) \tag{9}$$

The corresponding time series of differential terminal voltage with time lag of 3 cycles is expressed as:

$$\Delta V_L(j) = V_L(j) - V_L(j-3) \tag{10}$$

where the $V_L(j)$ is the average terminal voltage value at the jth cycle.

Since the average terminal voltage progressively increases during the switch turn-off period and decreases progressively during the switch turn-on period, a proportional function $P(j)$ is used to express this feature. $P(j)$ is experimentally set to be 1 for the first cycle after switching, 2 for the second cycle, and 3 for the third cycle for enhancement of the voltage progressive varying trends after

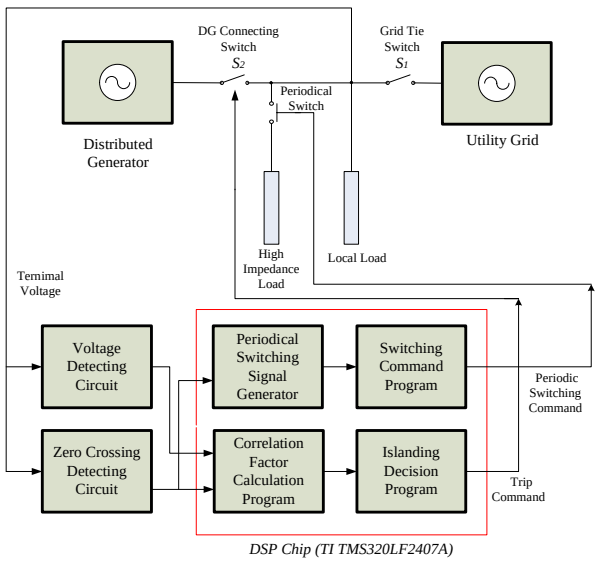

Fig.5 System configuration of the correlation factor islanding detector

switching on and off. The correlation factor between $\Delta S(j)$ and $\Delta V_L(j)$ is expressed as follows:

$$F_k = \frac{1}{N} \sum_{k=j-N}^{j} \Delta V_L(k) \times \Delta S(k) \times P(k) \qquad (11)$$

where F_k is the proposed correlation factor, as an islanding detection index, N is the number of cycles of the observing window, and N is set as 6 in this paper.

As described previously, in normal operation the correlation between $\Delta V_L(j)$ and $\Delta S(j)$ is weak and F_k is much lower than a threshold value. In contrast, as islanding occurs, $\Delta V_L(j)$ and $\Delta S(j)$ have a strong correlation and F_k becomes significantly larger than that in normal operation [22]. Through the proposed scheme, the correlation factor can be used as an islanding detection index and serves as a useful reference to activate the protective relays.

Fig. 6 depicts the procedure of the correlation factor method. It consists of zero crossing detection, periodical switching command generation, terminal voltage detection, correlation factor calculation, and decision process. The DSP measures the value of terminal voltage over 6 cycles, so that it avoids the impacts of various load variations and real power or reactive power disturbances. As shown in Fig. 6, a threshold for the islanding detection correlation factor is defined; the threshold is set to be 36 in this paper. Computer simulations were performed, and the simulation results of the variation of the correlation factor F_k before and after the islanding operation are shown in Fig. 7. As shown in Fig.7, if the islanding fault is occurring at the 6th cycle, then the correlation factor F_k increases during the next 6 cycles. At the 12th cycle the correlation factor F_k larger than the threshold *Top* F_k, and the islanding has been detected.

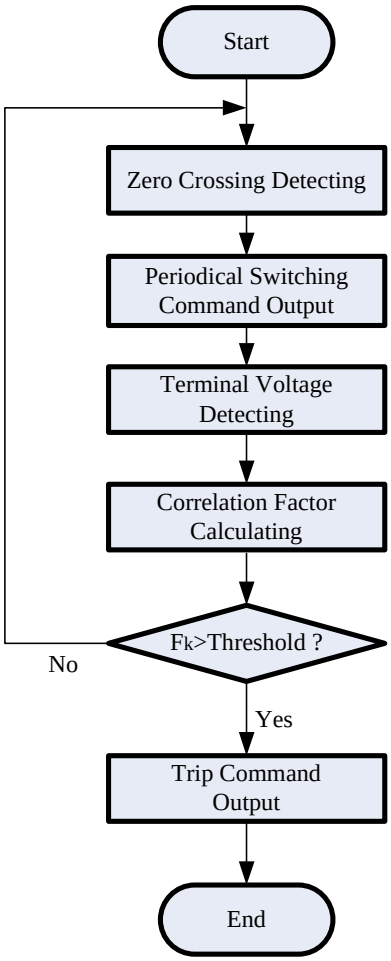

Fig. 6 Procedure of the correlation factor method

4 Experimental Results

To verify the proposed method, experiments were conducted to demonstrate its effectiveness of the islanding detection approach. The experimental tests were carried out on two kinds of generators: synchronous generator and induction generator. The procedures of the tests are to verify that the DG systems cease to energize the utility grid as specified in IEEE Standard 1547 when an unintentional island condition is present.

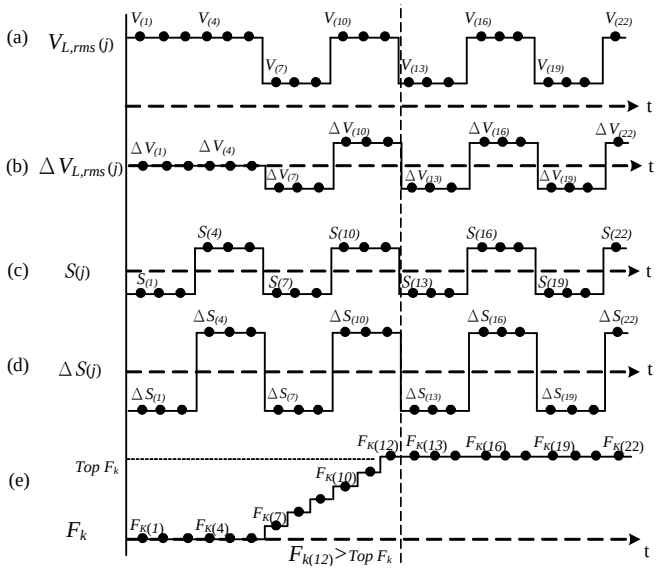

Fig.7 The simulation of the variation of F_k before and after the islanding operation

4.1 Islanding test for synchronous generators

The generation system employed in the islanding tests for synchronous generator consisted of a grid-interconnected, three-phase, 220V, 300W synchronous generator driven by a DC motor with 4 types of loads, including (a) maximum real load at unity power factor, (b) maximum real load at rated power factor lagging, (c) maximum real load at rated power factor leading, and (d) minimum load at unity power factor. The test circuit, specified in IEEE Standard 1547, is configured as shown in Fig. 8. The DG was started, synchronized to the utility grid, and then the tie-switch S_2 was closed to interconnect the DG to the grid. Open switch S_1 and record the time between the opening of switch S_1 and when the DG ceases to energize the load. Repeat test to 4 types of loads for a total of 5 times. The test is successful when the DG ceases to energize the test load within the timing requirements of IEEE Standard 1547 after switch S_1 is opened.

The effectiveness of the correlation factor method for synchronous generator has been validated in the experiments. The test results for 4 types of loads are shown in Table 1. The testing results show that the correlation factor, used as an index of islanding detection, can detect the islanding operation easily and accurately. The verification results also reveal that the proposed correlation factor method detected the islanding event with a maximum delay time of 0.19 seconds in the 20 tests for 4 types of loads. The average detection time of the 20 tests is 0.145 seconds. The detection time needed is much less than the maximal 2 seconds as specified by IEEE standard 1547.

In the typical test for the type (a) load, as shown in Fig. 9 of the typical test for the resistive load as an instance, the detection signal for islanding was issued in 0.158 seconds (totally 9.5 cycles for estimating the differential voltage magnitudes were needed) after the islanding operation started.

In the typical test for the type (b) load, as shown in Fig. 10, the detection signal for islanding was given in 0.15 seconds (totally 9 cycles needed) after the islanding operation started.

Table 1 Islanding test results of synchronous generator

Load combinations	Average trip time (ms)	Maximum trip time (ms)	Minimum trip time (ms)	Success times
(a)	149.6	191	109	5
(b)	157.8	187	136	5
(c)	121.28	183	44	5
(d)	150	168	92	5

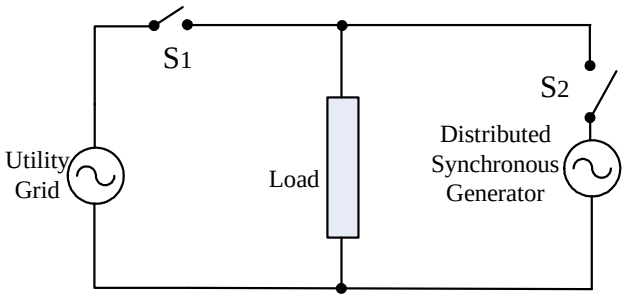

Fig.8 The islanding test configuration for synchronous generators

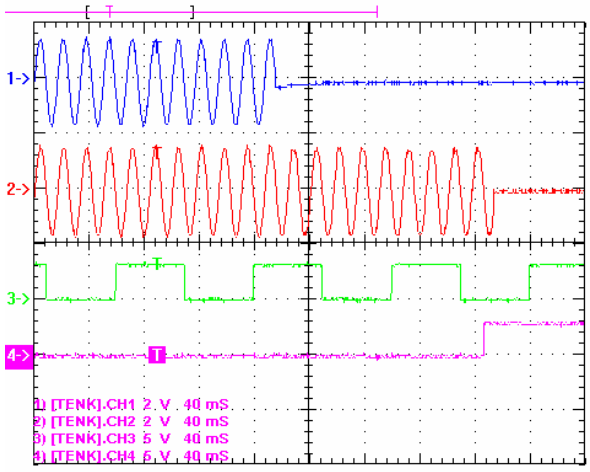

CH1:400V/div, CH2:400V/div, CH3:5V/div, CH4:5V/div, Time:40ms/div

Fig.9 The results of the experiment for synchronous generator using type (a) load

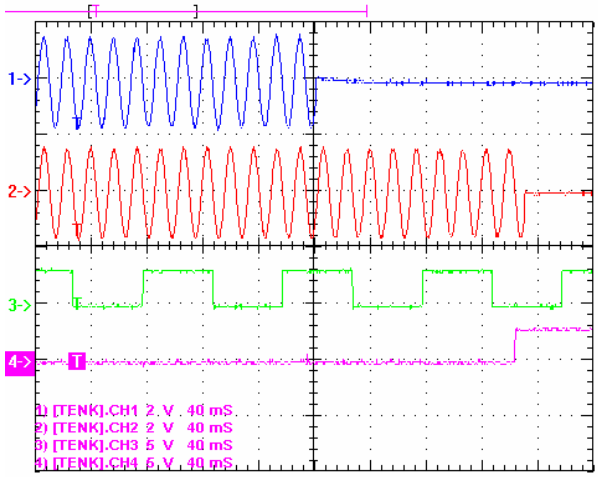

CH1:400V/div, CH2:400V/div, CH3:5V/div, CH4:5V/div, Time:40ms/div

Fig.10 The results of the experiment for synchronous generator using type (b) load

In the typical test for the type (c) load, as shown in Fig. 11, the detection signal for islanding was likewise announced successfully in 0.183 seconds (totally 11 cycles needed) after the islanding operation started.

In the typical test for the type (d) load, as shown in Fig. 12, the detection signal for islanding was likewise announced successfully in 0.158 seconds (totally 9.5 cycles needed) after the islanding operation started.

In Figs. 9 to 12, Channel 1 denotes the waveform of grid voltage (400V/div), Channel 2 indicates the waveform of local load terminal voltage (400V/div), Channel 3 depicts the switching signal of periodical electronic switch (5V/div) and Channel 4 shows the tripping signal (5V/div).

The capability of the proposed system to avoid false alarms was verified through the experiments of randomly switching the loads. The random load switching tests were taken 200 times for each type of load; results depict that no false alarm occurred out of the 800 switching tests. As an example of the typical test for the load at unity power factor, Fig. 13 exhibits that the detection system does not have false alarms due to the load switching.

In Fig. 13, Channel 1 denotes the waveform of grid voltage (400V/div), Channel 2 indicates the waveform of load current (1A/div), Channel 3 depicts the switching signal of periodical electronic switch (5V/div) and Channel 4 shows the tripping signal (5V/div).

To further evaluate the impact on the power quality due to the periodical voltage fluctuation injection by using the correlation factor method, three power quality indices were measured through a power quality analyzer. The three power quality indices evaluated were total harmonic distortion (THD), voltage fluctuation (P_{ST}) and three phase unbalance. Comparison results between with and without the voltage fluctuation injection are given in Table 2. The table shows that in normal operation of

Table 2 Impact on the power quality by voltage fluctuation injection (synchronous generator)

Condition	Power quality index	Phase		
		A	B	C
With voltage fluctuation injection	THD	0.8%	0.6%	0.6%
	PST	0.40	0.40	0.50
	3ϕ unbalance	0.4%		
Without voltage fluctuation injection	THD	0.7%	0.6%	0.6%
	PST	0.32	0.32	0.47
	3ϕ unbalance	0.5%		

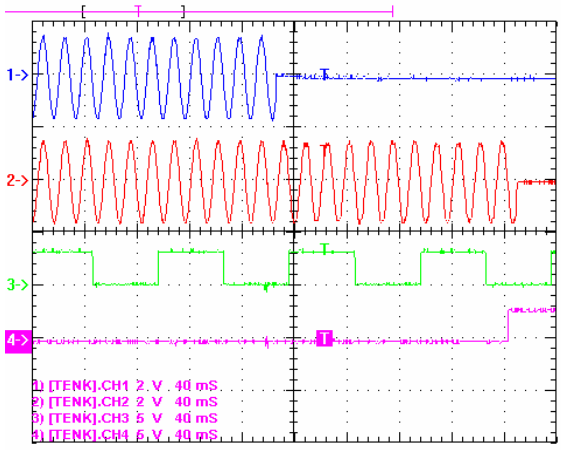

CH1:400V/div, CH2:400V/div, CH3:5V/div, CH4:5V/div, Time:40ms/div

Fig.11 The results of the experiment for synchronous generator using type (c) load

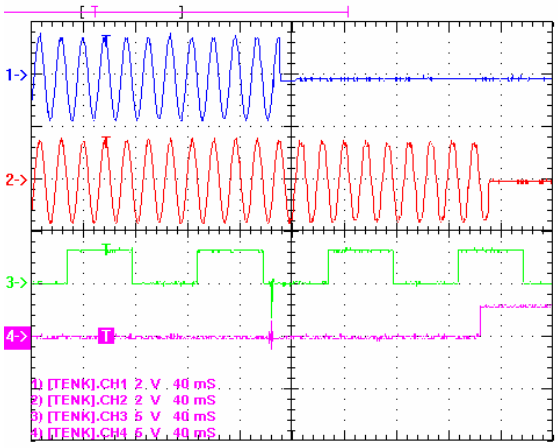

CH1:400V/div, CH2:400V/div, CH3:5V/div, CH4:5V/div, Time:40ms/div

Fig.12 The results of the experiment for synchronous generator using type (d) load

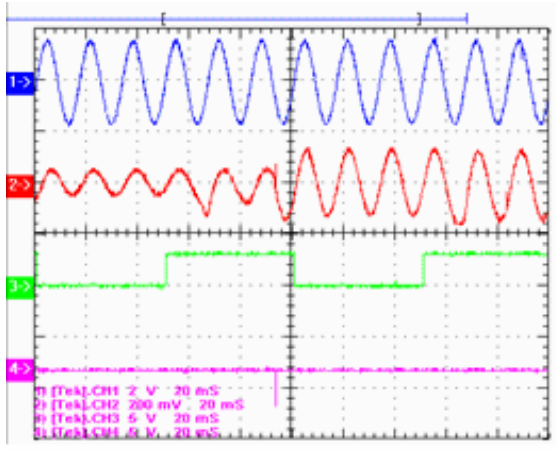

CH1:400V/div, CH2:400V/div, CH3:5V/div, CH4:5V/div, Time:20ms/div

Fig.13 The results of the experiment for random switching of the load

synchronous generator interconnected with the utility grids, though the high-impedance load switching occurred at the grid-interconnected point, the terminal voltage almost was not influenced. The differences between with and without the voltage fluctuation injection as shown in Table 2 are supposed to result from errors or noise from the measurement instrument.

4.2 Islanding test for induction generators

The generation system employed in the islanding tests for induction generator consisted of a grid-interconnected, three-phase, 220V, 300W induction generator driven by a DC motor with 3 types of loads, including (a) 33% rated load at unity power factor, (b) 100% rated load at unity power factor, (c) 120% rated load at unity power factor. The test circuit, specified in IEEE Standard 1547, is configured as shown in Fig. 14. The DG was started, synchronized to the utility grid, and then the tie-switch S_2 was closed to interconnect the DG to the utility grid. Adjust the islanding RLC load circuit in Fig. 14 to provide a quality factor of 1.0 ± 0.05. The reactive load is balanced so that the resonant frequency of the island circuit is within the under-frequency (59.5Hz) and over-frequency (60.5Hz) trip settings of the DG and as close to nominal frequency (60Hz) as possible. Open switch S_1 and record the time between the opening of switch S_1 and when the DG ceases to energize the load. Repeat test for 3 types of loads for a total of 5 times. The test is successful when the DG ceases to energize the test load within the timing requirements of IEEE Standard 1547 after switch S_1 is opened.

The effectiveness of the correlation factor method for induction generator has been validated in the experiments. The test results for 3 types of loads are shown in Table 3. The testing results show that the correlation factor, used as an index of islanding detection, can detect the islanding operation easily and accurately. The verification results also reveal that the proposed correlation factor method detected the islanding event with a maximum delay time of 0.216 seconds in the 15 tests for 3 types of load combinations. The average detection time of the 15 tests is 0.11 seconds. The detection time needed is much less than the maximal 2 seconds as specified by IEEE standard 1547.

In the typical test for the type (a) load, as shown in Fig. 15, the detection signal for islanding was issued in 0.117 seconds (totally 7 cycles for estimating the differential voltage magnitudes were needed) after the islanding operation started.

In the typical test for the type (b) load, as shown in Fig. 16, the detection signal for islanding was likewise announced successfully in 0.142 seconds (totally 8.5 cycles needed) after the islanding operation started.

In the typical test for the type (c) load, as shown in Fig. 17, the detection signal for islanding was likewise announced successfully in 0.15 seconds (totally 9 cycles needed) after the islanding operation started.

In Figs. 15 to 17, Channel 1 denotes the waveform of grid voltage (400V/div), Channel 2 indicates the waveform of local load terminal voltage (400V/div), Channel 3 depicts the switching signal of periodical electronic switch (5V/div) and Channel 4 shows the tripping signal (5V/div).

To further evaluate the impact on the power

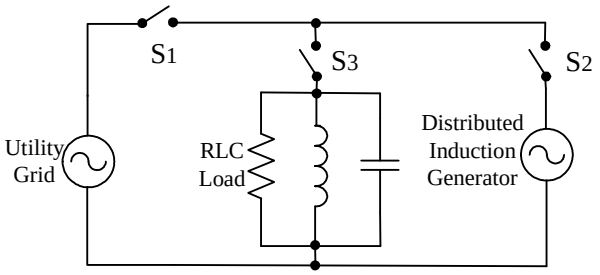

Fig.14 The islanding test configuration for induction generators

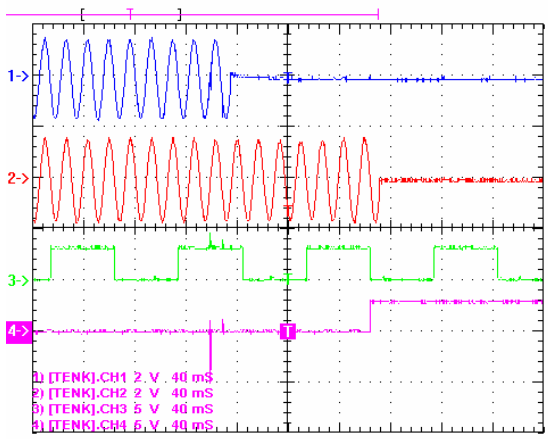

CH1:400V/div, CH2:400V/div, CH3:5V/div, CH4:5V/div, Time:40ms/div

Fig.15 The results of the experiment for induction generator using type (a) load

Table 3 Islanding test results of induction generator

Load Type	Average trip time (ms)	Maximum trip time (ms)	Minimum trip time (ms)	Success times
(a)	81.7	125	60.8	5
(b)	138.8	216	76	5
(c)	109.1	166	58.4	5

quality due to the periodical voltage fluctuation injection by using the correlation factor method, three power quality indices were measured through a power quality analyzer. Comparison results between with and without the voltage fluctuation injection are given in Table 4. The table shows that in normal operation of induction generator interconnected with the utility grids, though the high-impedance load switching occurred at the grid-interconnected point, the terminal voltage almost was not influenced. The differences between with and without the voltage fluctuation injection as shown in Table 4 are supposed to result from errors or noises of the measurement instrument.

5 Conclusions

Based on a correlated voltage fluctuation scheme, this paper has proposed a new method to quickly and reliably detect islanding operation of a DG system. The voltage fluctuation is injected on to the grid-interconnected point by switching a high-impedance load periodically. Observing the correlation factor of the proposed scheme through a digital signal processor, discrimination between islanding and other non-islanding disturbances can thus be made accurately.

To verify the effectiveness of the proposed technique, results obtained from experiments were used in this paper. The experimental results show that the proposed index of the islanding detection correlation factor can detect the islanding operation satisfactorily for different types of loads within 0.216 seconds. The detection performance is shown to be less dependent on load quality factor and power level. Besides, the test results also reveal that the new proposed method is easier and more economical for implementation as compared to the existing active detection approaches.

The directions for future research of the islanding detection method can be described as follow: To further improve the detection performance of the proposed active islanding detection method, the passive islanding detection methods that detect the islanding operation of DG by monitoring the selected power system parameters will be investigated and integrated in the proposed active method. Besides, for the passive islanding detection methods, there are many power system parameters to be monitored, such as voltage magnitude, the change rate of frequency, phase displacement, and power output. The using of optimization search methods, such as genetic algorithm or neural networks, for the best combination selection of the selected power system parameters will be investigated in the passive islanding detection method.

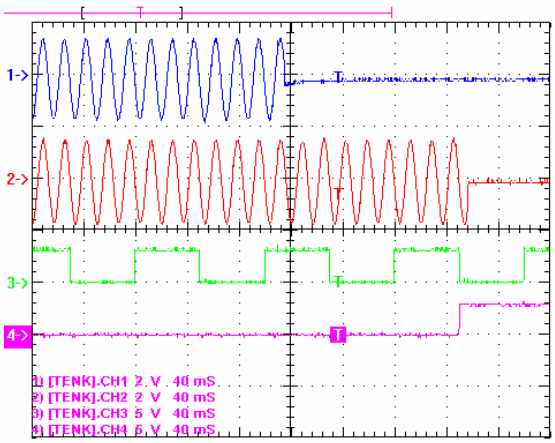

CH1:400V/div, CH2:400V/div, CH3:5V/div, CH4:5V/div, Time:40ms/div

Fig.16 The results of the experiment for induction generator using type (b) load

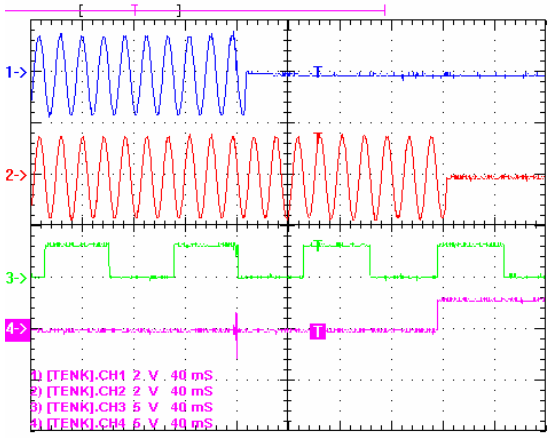

CH1:400V/div, CH2:400V/div, CH3:5V/div, CH4:5V/div, Time:40ms/div

Fig.17 The results of the experiment for induction generator using type (c) load

Table 4 Impact on the power quality by voltage fluctuation injection (induction generator)

Condition	Power quality index	Phase		
		A	B	C
With voltage fluctuation injection	THD	0.5%	0.5%	0.5%
	P_{ST}	0.29	0.17	0.26
	3ϕ unbalance	0.4%		
Without voltage fluctuation injection	THD	0.6%	0.7%	0.8%
	P_{ST}	0.24	0.18	0.19
	3ϕ unbalance	0.5%		

Acknowledgements

The author would like to express his acknowledgements to the National Science Council of ROC for the financial support under Grant No. NSC 95-2221-E-129-012.

References:

[1] V.E. Santos, A.G. Martins, and C.H. Antunes, A Multi-Objective Model for Sizing and Placement of Distributed Generation, *WSEAS Transactions on Power Systems*, Volume 1, Issue 7, 2006, pp. 1267-1272.

[2] Y.G. Hegazy and M.A. Mostafa, Reliability Indices of Electrical Distributed Generation Systems, *WSEAS Transactions on Systems*, Volume 4, Issue 10, 2005, pp. 1785-1790.

[3] A.H. Mantawy and M. Al-Muhaini, A New Particle-Swarm-Based Algorithm for Distribution System Expansion Planning Including Distributed Generation, *Proceedings of the 2nd IASME/WSEAS International Conference on Energy & Environment*, (EE'07), Portoroz, Slovenia, 2007, pp.236-241.

[4] M.H. Aliabadi, M. Mardaneh, and B. Behbahani, Siting and Sizing of Distributed Generation Unit Using GA and OPF, *Proceedings of the 2nd WSEAS International Conference on Circuits, Systems, Signal and Telecommunications*, (CISST'08), Acapulco, Mexico, 2008, pp. 202-206.

[5] T.H. Chen, M.S. Wang, and N.C. Yang, Impact of Distributed Generation on Voltage Regulation by ULTC Transformer using Various Existing Methods, *Proceedings of the 7th WSEAS International Conference on Power Systems*, Beijing, China, 2007, pp. 158-163.

[6] A.S. Bretas and R.H. Salim, A New Fault Location Technique for Distribution Feeders with Distributed Generation, *WSEAS Transactions on Power Systems*, Volume 1, Issue 5, 2006, pp. 894-900.

[7] K. Maki, S. Repo, and P. Jarventausta, Protection Coordination to Meet the Requirements of Blinding Problems Caused by Distributed Generation, *WSEAS Transactions on Circuits and Systems*, Volume 4, Issue 7, 2005, pp. 674-683.

[8] D. Ardito, S. Conti, N. Messina, and S. Nicotra, Operating Conflicts in Distribution Networks Protection with Distributed Generation, *WSEAS Transactions on Circuits and Systems*, Volume 4, Issue 9, 2005, pp. 1034-1042.

[9] G. Dalke, et al., Application of Islanding Protection for Industrial and Commercial Generators – an IEEE Industrial Application Society Working Group Report, *Proceedings of the 59th Annual Conf. Protective Relay Engineers*, Texas, USA, 2006, pp. 152-163.

[10] IEEE Std. 1547, *Standard for Interconnecting Distributed Resources with Electric Power Systems*, 2003.

[11] J.C.M. Vieira, D.S. Correa, W. Freitas, and W. Xu, Performance Curves of Voltage Relays for Islanding Detection of Distributed Generators, *IEEE Transactions on Power Systems*, Vol. 20, No. 3, 2005, pp.1660-1662**.**

[12] C.M. Affonso, W. Freitas, W. Xu, L.C.P. da Silva, Performance of ROCOF Relays for Embedded Generation Applications, *IEE Proceedings – Generation Transmission Distribution*, Vol. 152, No. 1, 2005, pp.109-114.

[13] W. Freitas, Z. Huang, W. Xu, A Practical Method for Assessing the Effectiveness of Vector Surge Relays for Distributed Generation Applications, *IEEE Transactions on Power Delivery*, Vol. 20, No. 1, 2005, pp.57-63**.**

[14] S.I. Jang, K.H. Kim, An Islanding Detection Method for Distributed Generations Using Voltage Unbalance and Total Harmonic Distortion of Current, *IEEE Transactions on Power Delivery*, Vol. 19, No. 2, 2004, pp. 745–752.

[15] M.A. Redfern, O. Usta, G. Fielding, Protection Against Loss of Utility Grid Supply for a Dispersed Storage and Generation Unit, *IEEE Transactions on Power Delivery*, Vol.8, No.3, 1993, pp. 948–954.

[16] F.S Pai, S.J. Huang, A Detection Algorithm for Islanding-Prevention of Dispersed Consumer-Owned Storage and Generating Units, *IEEE Transactions on Energy Conversion*, Vol. 16, No. 4, 2001, pp.346–351.

[17] S.K. Salman, D.J. King, G. Weller, New Loss of Mains Detection Algorithm for Embedded Generation Using Rate of Change of Voltage and Changes in Power Factors, *Proceedings of the 7th IEE International Conference on Developments in Power System Protection*, Amsterdam, Netherlands, 2001, pp. 82–85.

[18] S.I. Jang, K.H. Kim, Development of a Logical Rule-Based Islanding Detection Method for Distributed Resources, *Proceedings of the 2002 IEEE Power Engineering Society Winter Meeting*, New York, USA, 2002, pp. 800-806.

[19] J.W. Warin, Loss of Mains Protection, *Proceedings of the ERA Conference on Circuit Protection for Industrial and Commercial*

Installations, Landon, UK, 1990, pp. 4/3/1–12.

[20] P. Du, J.K. Nelson, Z. Ye, Active Anti-Islanding Schemes for Synchronous-Machine-Based Distributed Generators, *IEE Proceedings – Generation Transmission Distribution*, Vol.152, No.5, 2005, pp.597-606.

[21] P.D. Hopewell, N. Jenkins, A.D. Cross, Loss-of-Mains Detection for Small Generators, *IEE Proceedings –Electrical Power Application*, Vol. 143, No. 3, 1996, pp.225-230.

[22] W.Y. Chang, H.T. Yang, An Active Islanding Protection Method for Distributed Synchronous Generators, *Proceedings of the 7th IET International Conference on Advances Power System Control, Operation and Management*, Hong Kong, China, 2006, Paper No. APSCOM2006-128.